N O T I C E

THIS DOCUMENT HAS BEEN REPRODUCED FROM
MICROFICHE. ALTHOUGH IT IS RECOGNIZED THAT
CERTAIN PORTIONS ARE ILLEGIBLE, IT IS BEING RELEASED
IN THE INTEREST OF MAKING AVAILABLE AS MUCH
INFORMATION AS POSSIBLE

DESIGN AND CONSTRUCTION OF A "FARADAY CUP"
FOR MEASUREMENT OF SMALL ELECTRONIC CURRENTS

Andre Veyssiere

NATIONAL AERONAUTICS AND SPACE ADMINISTRATION
WASHINGTON D.C. 20546   SEPTEMBER 1985

STANDARD TITLE PAGE

1. Report No. NASA TM-77915	2. Government Accession No.	3. Recipient's Catalog No.
4. Title and Subtitle DESIGN AND CONSTRUCTION OF A "FARADAY CUP" FOR MEASUREMENT OF SMALL ELECTRONIC CURRENTS		5. Report Date September, 1985
		6. Performing Organization Code
7. Author(s) Andre Veyssiere		8. Performing Organization Report No.
		10. Work Unit No.
9. Performing Organization Name and Address SCITRAN Box 5456 Santa Barbara, CA 93108		11. Contract or Grant No. NASw 4004
		12. Type of Report and Period Covered Translation
12. Sponsoring Agency Name and Address National Aeronautics and Space Administration Washington, D.C. 20546		14. Sponsoring Agency Code

15. Supplementary Notes

Translation of "Etudes et Realisation d'une 'Coupe de Faraday' pour les Mesures de Faibles Courants Electroniques", Commissariat a l'Energie Atomique, Saciay (France) Centre d'Etudes Nuclearies. October, 1967. pages 1-28, Report. CEA-R-3276. (N68-25321)

16. Abstract

The design of a device for measuring and integrating very small currents generated by the impact of a charged particle beam upon a Faraday cut is described. The main component is a graphite bloc capable of stopping practically all the incident changes. The associated electronic apparatus required to measure better than 10^{-13} ampere with a precision of 1 per cent is also described.

17. Key Words (Selected by Author(s))	18. Distribution Statement
	Unclassified and Unlimited

19. Security Classif. (of this report) Unclassified	20. Security Classif. (of this page) Unclassified	21. No. of Pages 33	22. Price

Saclay Center of Nuclear Studies

Department of Physics Research

DESIGN AND CONSTRUCTION OF A "FARADAY CUP"

FOR MEASUREMENT OF SMALL ELECTRONIC CURRENTS

by

Andre Veyssiere

October 1967

1 - INTRODUCTION

In the photonuclear experiments performed with monochromatic γ coming from the in-flight annihilation of positrons [1;2;3] it is necessary to measure the electric currents that produce these photons, if not in an absolute respect, at least with a certain degree of fidelity.

The purpose of this report is to describe the design and construction of a measuring system enabling a degree of precision of 1% in the measurement of electronic currents less than 10^{-13} Ampere. The particles in the beam have energies between 10 and 60 MeV.

* Throughout this article the term electron designates both the negative particle (negatron) as well as the positive particle (positron).

---

*Numbers in margin indicate foreign pagination

The report is composed of two parts: the first part, which is the largest, describes the charge detector (Faraday cup), and the second part describes the electronic equipment itself and also provides some experimental results.

II - <u>PRIMARY CHARACTERISTICS OF A "FARADAY CUP"</u>

By deciding upon the degree of accuracy for the measurement in the preceding paragraph, we defined the percentage of the charge that we can allow to escape from the detector.

Several phenomena can disturb the precise measurement of the number of charges:

a) Charges escaping after having traveled through the body of the detector.

b) Charges escaping by secondary emission or backscattering.

c) Foreign charges are detected (for example: collection of particles coming from the ionization of the gas surrounding the detector).

d) Since the currents to be measured are very small the detector must have a very high leakage resistance with respect to ground, but must not be sensitive to external electrostatic phenomena.

In the following paragraphs we are going to study each of these points and attempt to minimize their effects.

III - STUDY OF DISTURBING PHENOMENA

III - A/- Escape of Charges After Traveling Through the Detector

We will make the most energetic particles (60 MeV) lose all their energy in the body of the "cup" and thus become easily detected by the medium. This energy loss comes about through ionization, by bremsstrahlung, and by annihilation in the case of positrons.

In the case of energy loss through ionization there is no problem: the energy is directly transferred to the material making up the detector and the particles cannot escape if the latter is thick enough. Unfortunately, in the cases of energy loss due to radiation and annihilation the photons created in turn produce particles that can escape: this phenomenon is the well-known avalanche effect.

In order to decrease this avalanche effect a material must be used in which the energy loss is produced as much as possible through ionization, and at the same time as little as possible through radiation. This is what will determine the choice of material.

III - A. -1) Choice of Material

If the critical energy Ec is defined as being the energy at which the electrons lose as much energy through ionization as through radiation, one can plot a curve (1) showing the variation in Ec as a function of Z [4]*. From this curve we can see that it is advantageous to choose an element at the beginning of the Mendeleieff table. Since we must work with

---

* As an initial approximation the critical energy Ec obeys the law of $\frac{800}{Z+1,2}$ MeV [5].

power levels of just a few mW we will take carbon which is a common element and is easy to work with.

At a high power level it would be better to use water, but the use of water brings up insulation problems that are hardly compatible with the measurement of small currents.

III/ -A/ -2) Calculation of the Energy Loss

To calculate the energy loss we start with a beam of 60-MeV positrons and we calculate the energy losses due to ionization, radiation and annihilation from slices of a thickness equal to 1g/cm².

The energy loss values by ionization and radiation are taken from the tables of Berger and Seltzer [5].

Calculation of the energy losses through ionization is made according to the Bethe theory by using the formulation of Rohrlich and Carlson:

$$\frac{1}{\rho}\left(\frac{dE}{dx}\right)_{col}^{\pm} = \frac{2\pi N_a \, r_0^2 \, mc^2}{\beta^2} \frac{Z}{A} \left\{ \left[\log_n \frac{\sigma^2(\sigma+2)}{2\left(\frac{I}{mc^2}\right)^2} \right] + F^{\pm}(\sigma) - \delta \right\} \qquad 4$$

$$F^{-}(\sigma) = 1 - \beta^2 + \left[\frac{\sigma^2}{8} - (2\sigma+1)\log_n 2 \right] \frac{1}{(\sigma+1)^2}$$

For the negatrons

$$F^{+}(\sigma) = 2 \log_n 2 - \frac{\beta^2}{12}\left[23 + \frac{14}{\sigma+2} + \frac{10}{(\sigma+2)^2} + \frac{4}{(\sigma+2)^3} \right] \quad \text{for the } e^+$$

For the positrons

The meanings of the various symbols are explained as follows:

mc^2 = rest energy = 0.511 MeV

$\mathbf{E}$ = kinetic energy in units of mc^2

β = v/c = $\dfrac{\sqrt{E(E+2)}}{E+1}$

Z = Atomic number

A = Atomic weight

ρ = Density

I = Average excitation energy = $Z(9.76 + 58.8\, Z^{-1.19})$ ev

δ = correction of the density effect

Na = Avogadro's number = 6.02×10^{23} electrons/mole

r_0^2 = $\left(\dfrac{e^2}{mc^2}\right)^2 = 7.94 \; 10^{26}\, cm^2$

Curves 2 show these values for graphite.

The losses due to annihilation are calculated with respect to the bremsstrahlung losses taken from the preceding tables.

Indeed, we know [6] that the number of photons produced by the annihilation process per g/cm^2 of material obeys the following law:

$$P = 2\pi\, r_0^2 \frac{1}{E^+}\Big[(\log_n 2E^+) - 1\Big]\frac{Na\, Z}{A}$$

for a simple body with:

E^+ = Total energy of the positrons expressed in $m_0 c^2$

Na = Avogadro's number

r_0 = radius of the electron.

Whereas the energy loss by bremsstrahlung per unit of length obeys the following law [7]:

$$\left(\frac{dE}{dz}\right)^{\pm} = 4 Z^2 \frac{N E_c}{137}\, r_0^2 \, \log_n(183\, Z^{-1/3})$$

5

with E_c being the kinetic energy of the electrons (E_c^+ E_c^-)

N the number of atoms/cm³.

By replacing the parameters with their numerical values for graphite (ρ = 1.8 g/cm³: Z = 6; A = 12) and by reducing the two equations to comparable units, we finally obtain the ratio α

$$\alpha = \frac{\text{Energy loss due to radiation}}{\text{Energy loss due to annihilation}}$$

$$\alpha \neq 0{,}128 \frac{E_c^+}{\left[\text{Log}_n 2 (E_c+1) - 1 \right]}$$

with E_c^+ = kinetic energy of the positrons expressed in units of $m_0 c^2$.

This procedure is justified by the fact that the two formulae have nearly the same approximations and that, at any rate, a rough value is sufficient because the losses due to annihilation only represent a few percentage points of the total loss.

Lastly, we find that we need about 15 centimeters of graphite to completely absorb the energy of the positrons (to a maximum of 60 MeV). The distribution of energy losses is as follows:

6

- Losses due to ionization = 75%
- Losses due to radiation = 20%
- Losses due to annihilation = 5%

As for the negatrons the calculation shows that a few extra millimeters are necessary: the larger amount of loss due to ionization

almost compensates for the absence of the annihilation phenomenon [ref. 5 p. 31].

The energy spectrum of the γ extends over the entire range going from the maximum energy of the positrons (at the beginning of the graphite block) to an energy level of a few MeV at the end of the same block. It is therefore the γ having the most energy that have to travel through a greater thickness of material.

We will now calculate the energy distribution of the γ leaving the graphite block in which we will have taken into account the attenuation by making the following two pessimistic assumptions:

- The energy distribution of the bremsstrahlung gammas is constant from maximum energy to zero energy.

- The γ created by annihilation in a given slice of the material have the energy $E_\gamma = E_C^+ + 3/2\, m_0 c^2$, if E^C represents the energy of the electrons upon entering this slice.

Thus we obtain the distribution of the γ created in the graphite and at the outlet point.

TABLE I

Energy spectrum of the γ MeV		$N\gamma_C$	$N\gamma$
60	50	2,5 %	1,9 %
50	40	3 %	2,3 %
40	30	4 %	3,25 %
30	20	4,5 %	3,75 %
20	10	6 %	5,2 %
<10		5 %	4,4 %

$N\gamma_C$ represents the percentage of energy of the γ created in the graphite in relation to the total incident energy.

$N\gamma$ represents the percentage of energy of the γ exiting the graphite in relation to the total incident energy.

<u>N.B.</u>: The energy of the γ are expressed by rounded-off figures, with the $3/2m_0c^2$ representing a negligible error our subsequent calculations.

III/ -A/ -3) <u>Absorption of the γ</u>

The gammas created in the graphite before leaving the block will obviously result in ion pairs and electrons through the Compton effect. These particles are likely to escape and distort the measurement of the current. It is therefore imperative to stop all the γ with a second material having a high Z value.

For reasons of practicality we chose Pb. The gammas in lead produce avalanches and the problem is to know how many electrons we can allow to escape and still remain within the desired limits of precision.

8

In order to evaluate the braking of the γ by avalanches we use the results of a theoretical study by R.R. Wilson [8]. The results obtained using a Monte Carlo method give the number of electrons present at a certain distance inside the material when the surface of the material has been struck by a γ or an electron.

Figure 3 shows one of these curves; the tail is easily extrapolated for the depths greater than 10 lengths of the radiation because it decreases according to an exponential law of the type $Ae^{-0,24\lambda}$ with λ being expressed in lengths of radiation.

Several tests induced us to use 20 lengths of radiation (about 105 mm) to have an escape probability of about $1\%_o$.

Our results are summarized in Table 2 herebelow:

E_γ MeV	N_γ	For 105 mm of Pb	
		Ne_1	Ne_T
60 50	1,9 %	0,025	$1,2 \ 10^{-4}$
50 40	2,3 %	0,02	$1,4 \ 10^{-4}$
40 30	3,25 %	0,015	$1,8 \ 10^{-4}$
30 20	3,75 %	0,01	$1,8 \ 10^{-4}$
<20	9,6 %	0,004	$3 \ 10^{-4}$

where E_γ represents the energy of the γ

N_γ represents the percentage of energy of the γ in relation to the total energy exiting the graphite.

Ne_1 represents the number of electrons present after 20 lengths of radiation in the lead when a gamma has given birth to an avalanche.

Ne_T represents the number of electrons present after 20 lengths of radiation in our case.

9

In conclusion we will take 15 cm of graphite with a density of 1.8 g/cm³ and 10.5 cm of lead for the primary braking of the particles. Other authors [9, 10] using somewhat different methods arrive at the same

results.

III - B/ - Secondary Emission and Backscattering

The limit between true secondary emission and backscattering is quite difficult to define; nevertheless, one can say that true secondary emission affects electrons emitted within an energy band ranging from a few electron volts to a few tens of electron volts and that beyond this range we are primarily dealing with backscattering [11, 12, 13, 14].

At any rate, it is to our advantage to use a material with a low Z value (which is the case in our use of graphite), to reduce as much as possible the angle of backscattering and, if possible, to trap the secondary particles with electric or magnetic fields, since the backscattered particles have very little energy anyway.

a) Secondary Emission

Secondary emission has been studied at the high energy levels that we are interested in with the primary objective of fabricating current monitors for particle accelerators. Since, as a general rule, these monitors are all made of aluminum and calibrated to primary monitors, we do not know with precision the efficiency levels of other substances [15, 10, 17, 18, 19, 20].

According to some values put forth by the previously quoted authors we can situate the secondary emission coefficient for graphite at around 1% between 1 and 100 MeV (range where we have a minimum). The angle of backscattering can be reduced very easily

by putting the graphite at the bottom of a well. In our work we reduced
the solid angle to $2\pi/12$ steradians creating a well 10 cm in diameter and
12.5 cm deep. This is compatible with the dimensions of our beam ($\emptyset$ = 5
cm).

b) Backscattering

Theoretical studies [2] and experimental studies [22] on this
phenomenon have shown that the coefficient of β re-emission is inversely
proportional to the energy of the incident electrons E_C and increases more
or less proportionally with the atomic number Z (except for slight values
of Z) of the scattering material. For graphite we chose, similarly to
other authors [23, 9] β = 0.006 for E_C = 10 MeV, which gives us $\beta \#$ 0.001
for 60 MeV. (The difference between the value of β for the incident
positrons and the value of β for the incident negatrons is sufficiently low
to be disregarded).

In addition, the number of electrons backscattered varies with
$\sin^2\delta$ with δ representing the half angle at the top of the cone in which
backscattering can occur). Moreover, this law is pessimistic for materials
with a small Z value.

Lastly, the ratio of the number of electrons that can be
re-emitted by backscattering to the number of primary electrons varies from
10^{-4} (for E_C = 60 MeV) to 5×10^{-4} for E_C = 10 MeV, with the dimensions of
our well being taken into account.

Furthermore, we inserted a permanent magnet into the walls of the
well, creating a diametral magnetic field of 50 gauss, which rejects
approximately all of the particles whose energy is less than 500 KeV [24].

We preferred the magnetic trap to the electric trap because it does not require any voltage supply systems that could be prejudicial to the insulation of the Detector.

N.B.: The phenomenon of nuclear elastic scattering to 180° is entirely negligible. Its effective cross section is about 10^{-32} cm^2 MeV^{-1}. S^{-1} [25].

c) Ionizat'on

It is necessary to enclose the body of the detector in a vacuum enclosure in order to reduce as much as possible the production of particles due to ionization. These ions are attracted by the detector because the detector is at the potential of the polarization value of the input tube of the measuring instrument.

For a constant current of particles arriving at the detector, curve no. 4 gives the current measured for different values of air pressure around the detector: (Curve taken from reference 9)
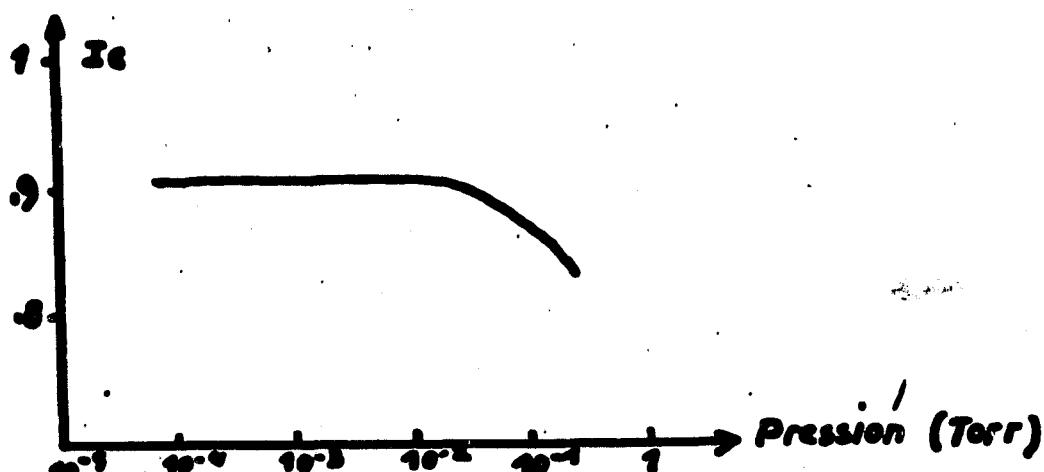
Figure 4 - Key to Figure 4 - 1: Pressure (Torr)

At this point it should be noted that the graphite commercially available (S = 1.6 to 1.8 g/cm³) degasses considerably and that it is very difficult to reach a vacuum level of 10^{-5} mm Hg. For this reason we had to leave the Faraday cup for two months while being vacuum pumped before being able to make precise measurements.

We connected the detector directly to the vacuum enclosure of the photon monochromatization system to avoid secondary emission and annihilation of positrons in the input window.

d) Shielding

The vacuum enclosure is made up of a stainless steel receptacle without a solution for electrical continuity and thus constituting a very good Faraday shield. The body of the detector weighing approximately 250 kgs is kept electrically insulated in this shield by sleeves of sintered aluminum oxide with a resistivity of about $10^{15}\Omega\,cm^2/cm$.

The output of the signal is made by a vacuum-tight leading-through made of glass with a large diameter and having a leakage resistance of > $10^{13}\Omega$.

IV - MECHANICAL CONSTRUCTION

The primary specifications have already been given during the design stage, at least as concerns the longitudinal dimensions. The transverse dimensions are established from the diameter of the well so that there is a thickness of graphite at least equal to the longitudinal thickness.

Figure 5 taken from the mechanical file gives the primary dimensions of the detector.

V - MEASUREMENT OF ELECTRONIC CURRENT

For our physics experiments we must know at any given time the electronic current creating monochromatic photons and the total number of charges that have fallen upon the detector during the entire duration of the operation. As these experiments are performed with a linear electron accelerator, we must take into account both the distance separating the detection point from the measurement point of the current, as well as

the high-frequency interference created by the power modulators. In addition, since the current drift of the electronic amplifier represents a non-negligible fraction of the lowest currents to be measured, it is necessary to add a device that takes this drift value into account (some 10^{-14}A).

Briefly put, the measurement system comprises (Figure no. 6)
- A DC amplifier including an input electrometer tube which, thanks to a counter reaction, tolerates relatively low leakage resistances [26]. Indeed, if Rf and RCR are the leakage counter-reaction resistances and A the gain of the amplifier, it is sufficient to have Rf $>>\frac{RCR}{A}$so that the voltage measured at the output is $V_S \approx$ I x RCR. In our case Rf $>10^{12}$, RCR$\leq 10^{11}$, A $>$ 5000.

This amplifier associated with an external galvanometer or digital voltmeter easily enables the measurement of 10^{-13}A (with RCR = $10^{11}\Omega$). This is the smallest current value that we have had to measure

throughout all of our operations.

- An integrator composed essentially of an "Integrating Digital Voltmeter" manufactured by Hewlett Packard which, thanks to the way in which it operates, completely eliminates high-frequency interference and integrates the voltage at the terminals over any period of time.

- A device that on the one hand sends the voltage output from the amplifier with either a + or - sign to the integrator, and on the other hand stops or starts the electron accelerator according to a rhythm determined by a clock. Measurement of the number of charges is then made in the following way:

    - Over a time interval T the integrator receives (with the accelerator operating) the voltage of the signal plus the drift voltage of the

zero level of the amplifier.

    - During the same time interval the integrator receives (with the accelerator now stopped) the drift voltage alone after inversion of the sign.

    Therefore, at the end of a time interval of 2T the value displayed on the integrator will effectively represent the integration of the signal alone. With the drift of the zero being slow we took a value of T = 1 minute.

Remark 1: Since the accelerator operates in pulses (duration: 1 μs ; repetition frequency: 1000 Hz) it is necessary to apply a time constant of about 1 second for the detector-amplifier assembly.

Remark 2: Although for the Faraday cup itself it is quite easy to only let $1\%_o$ of the detected charges escape, it is more difficult to measure the current with this same degree of accuracy. Indeed, we are dependent upon a DC electrometer-tube amplifier which needs to be used with extreme caution and calibrated quite frequently. It is very sensitive to temperature fluctuations and must be put in an isothermal enclosure; furthermore, the high resistances often undergo variations in their level with time and depending on the voltage applied to their terminals. It is therefore necessary to often check the value of the resistance with a bridge, and the response of the unit using a current generator as a reference. The measurement imprecision of the digital voltmeter (10^{-4}) does not have any incidence.

VI - EXPERIMENTAL RESULTS

The Faraday cup/amplifier/integrator assembly was mounted on a monochromatic photon production device designed by the photonuclear reaction design group of the Medium Energy Nuclear Physics Service [3] at the linear electron accelerator installation of Saclay.

15

We were unable to measure the efficiency of the system because, as it was not intended for the measurement of high currents, it was impossible to find a sufficiently precise monitor that would work in this range of power (cf. § III A 1).

However, we were able to:

- evaluate the angular acceptance of our system;
- calibrate the number of photons produced according to the

number of incident positrons;

- measure the yield in negatrons and positrons of the magnetic optical guidance converter ($e^{-} \longrightarrow e^{+}$) system of the electrons.

Before computation of these measurements we wish to review the layout of the photon production installation in Figure 7. The 45-MeV negatron beam coming from the linear accelerator after focusing falls upon a gold converter which produces ion pair electrons. These electrons are selected by a triplet lens T which gives a beam of monochromatic particles. The particles, when positrons, annihilate themselves partially on a target L made of a light material (Li) and give a beam of γ that will be used at point A. The unannihilated positrons are diverted by magnet M and detected by the Faraday cup.

VI - A/ - Angular Acceptance

When the target made of Li is removed, all the electrons go freely into the vacuum tube and are detected by the Faraday Cup under the focusing effect of the quadrupole lens Q_c. However, when target "L" is put in the beam it causes a divergence of the unannihilated positron beam and the Faraday Cup only detects a portion of it (which varies with the energy). It is very difficult to geometrically measure the acceptance angle because firstly

16

the beam is not punctual and secondly its path is disturbed by magnet M.

If we assume that the divergence of the beam is solely due to the multiple scattering in the lithium, we can calculate the percentage of

particles contained within an acceptance cone having a half angle at the top of θ_1 as a function of the energy [27, 28]. This percentage is expressed as follows:

$$P = 2 \int_0^{\theta_1} \frac{1}{\theta_0 \sqrt{2\pi}} \, e^{-\theta^2/2\theta_0^2} \, d\theta$$

with

$$\theta_0 = 2,3 \cdot 10^{-2} \frac{Z}{\sqrt{A}} \frac{\sqrt{M}}{E}$$

M in mg/cm²

E in MeV

θ_0 in radians

In our case (target made of Li) $\theta_0 = \frac{0.35}{E}$ radians; we standardize the theoretical curve and the experimental curve (Fig. 8) for the first point at 7.2 MeV which enables us to determine the angle θ_1 and to ascertain that the experimental curve does indeed obey the law of multiple scattering $\theta_1 \neq 0,025$ radians is found, a value that is perfectly compatible with our dimensions.

VI - B/ - Calibration of the number of photons produced as a function of the number of incident positrons.

Since we must know the exact number of photons that fall upon target A in order to establish the effective cross sections (Γn) of the bodies that we wish to study, it is imperative to know the correlation between the number of photons and the number of unannihilated positrons that fall upon the detector. To accomplish this a large crystal I Na is put in place of target A, followed by a photomultiplier [1, 2] that counts the γ while the detector current is measured. Unfortunately, in order to avoid stacking on the the γ sensor channel it is necessary to reduce the flow of γ and therefore measure a very small current at the detector. We are even forced to use an aluminum block

to attenuate the flow of γ in order to remain within the range of measurable current.

Figure 9 gives the number of monochromatic photons produced by the lithium target as a function of the energy of the incident positrons. For each point on the curve the number of positrons (after having traveled through the lithium target) falling on the detector was constant and equal to 0.88×10^{-9} Coulombs. This charge was obtained with a current of 2×10^{-13} Ampere over 1 1/2 hours. The accelerator was operating at 1000 cycles per second, which represents 1000 electrons per pulse. N.B.: Curve 9 was made taking into account the weakening due to the aluminum block and the efficiency of the sodium iodide crystal [29] (Figures 11 and 12).

VI - C/ - Efficiency of Negatron and Positron Production

It is interesting to know the maximum negatron and positron currents that one can hope to reach under particular operating conditions of the linear accelerator, which, furthermore, have already been measured on this installation when the accelerator was operating at 30 MeV [30]. At that time the current measurements were made with an ionization chamber [31].

In Figure 10 we give a result obtained with accelerator conditions that were not yielding maximum efficiency.

The conditions were:

Repetition frequency	1000 Hz
Duration of the pulse	$0.5\,\mu s$

MeV
Ec

vs Z

FIG. 1

Eau

1 Numéro atomique   atomic number

1
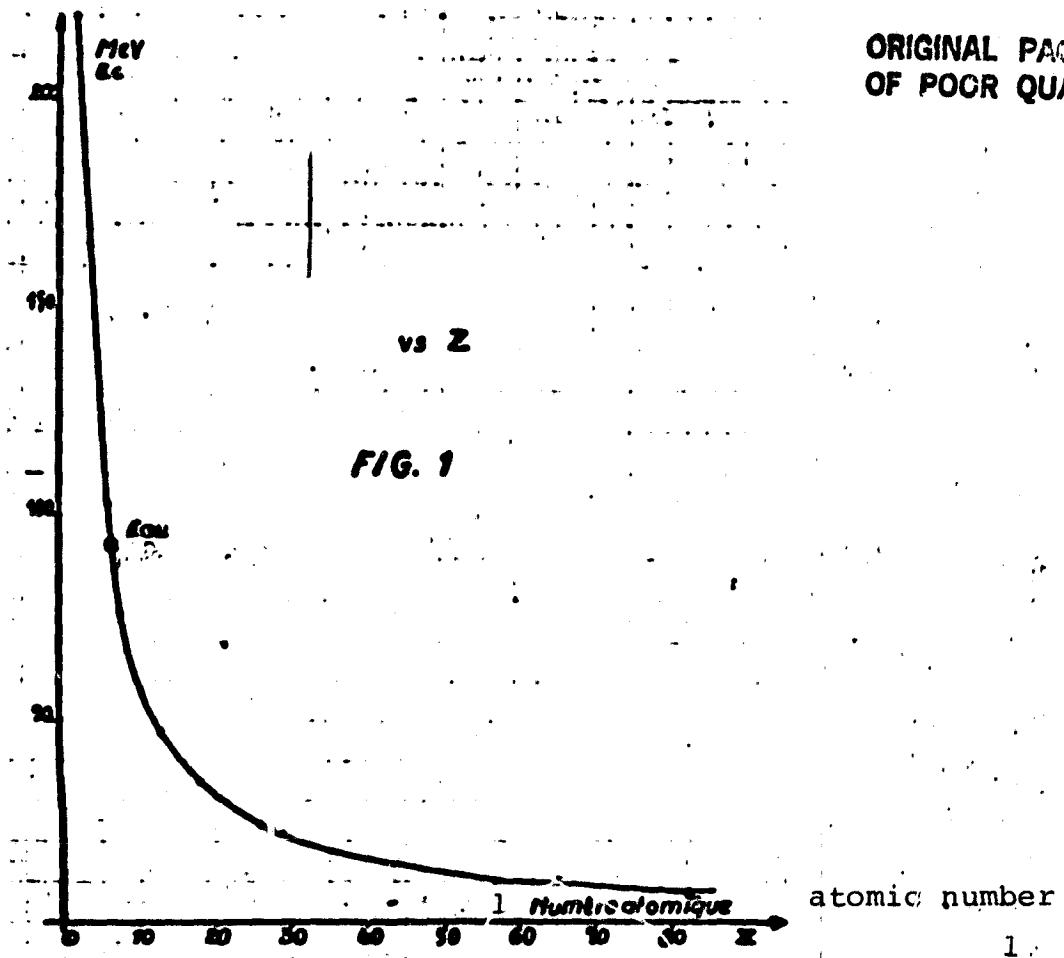
Fig 1 .Critical energy   vs z

MeV cm²·g⁻¹

1

PERTES D'ENERGIE
DES ELECTRONS
dans le
CARBONE

E 100

2

pertes par
rayonnement

FIG. 2

E 70   2a

3

pertes par ionisation

2b

Energie cinétique des électrons

4

1 energy losses
of electrons in carbon

2 radiation losses

3 ionization
        losses

4electron kinetic
        energy

100 KeV   1 MeV   10 KeV   100 MeV

20
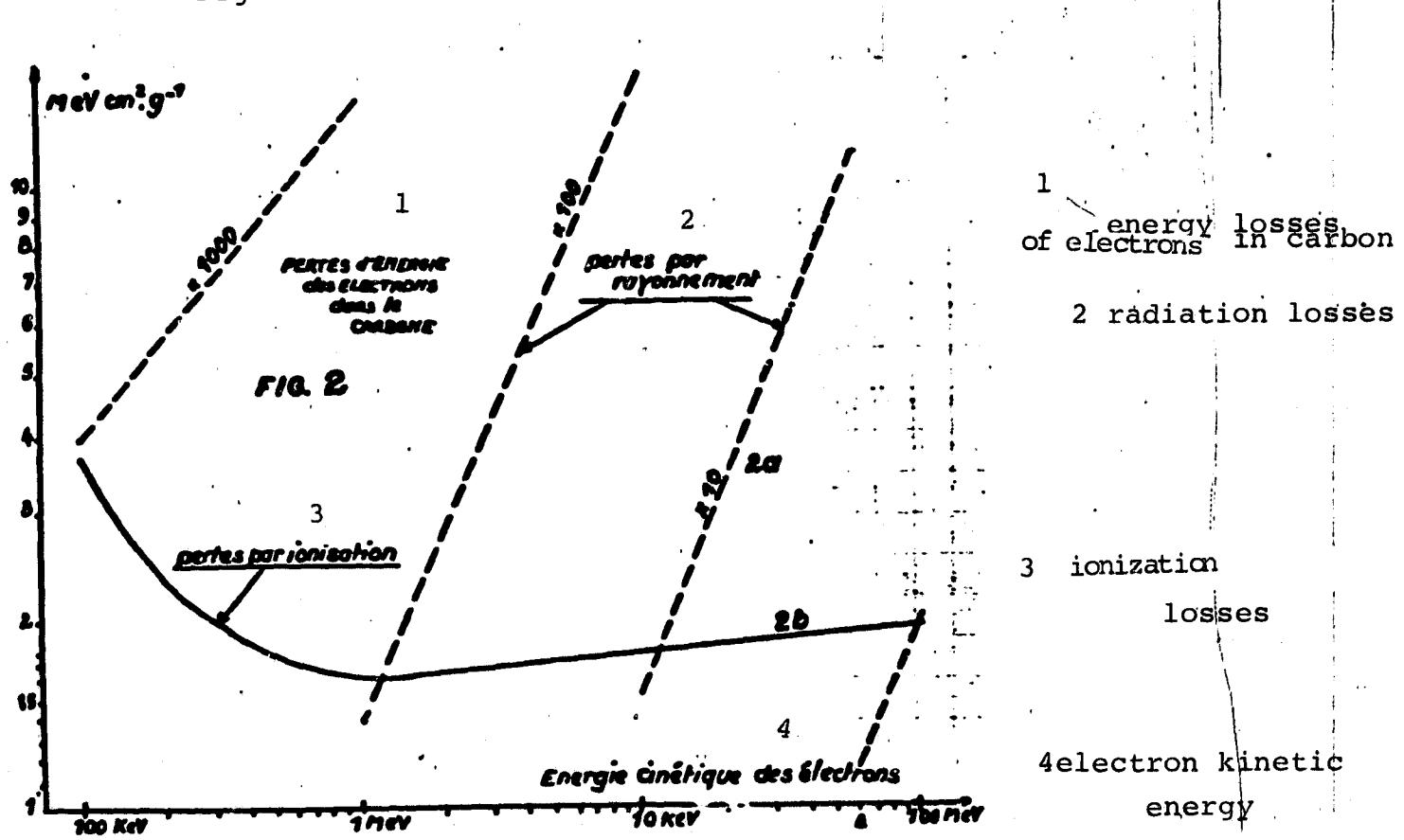
Peak current   100 mA

Conversion target   Gold

It is obvious that with these operating conditions the spectrum
of electrons was very wide since the filling time of the sections was
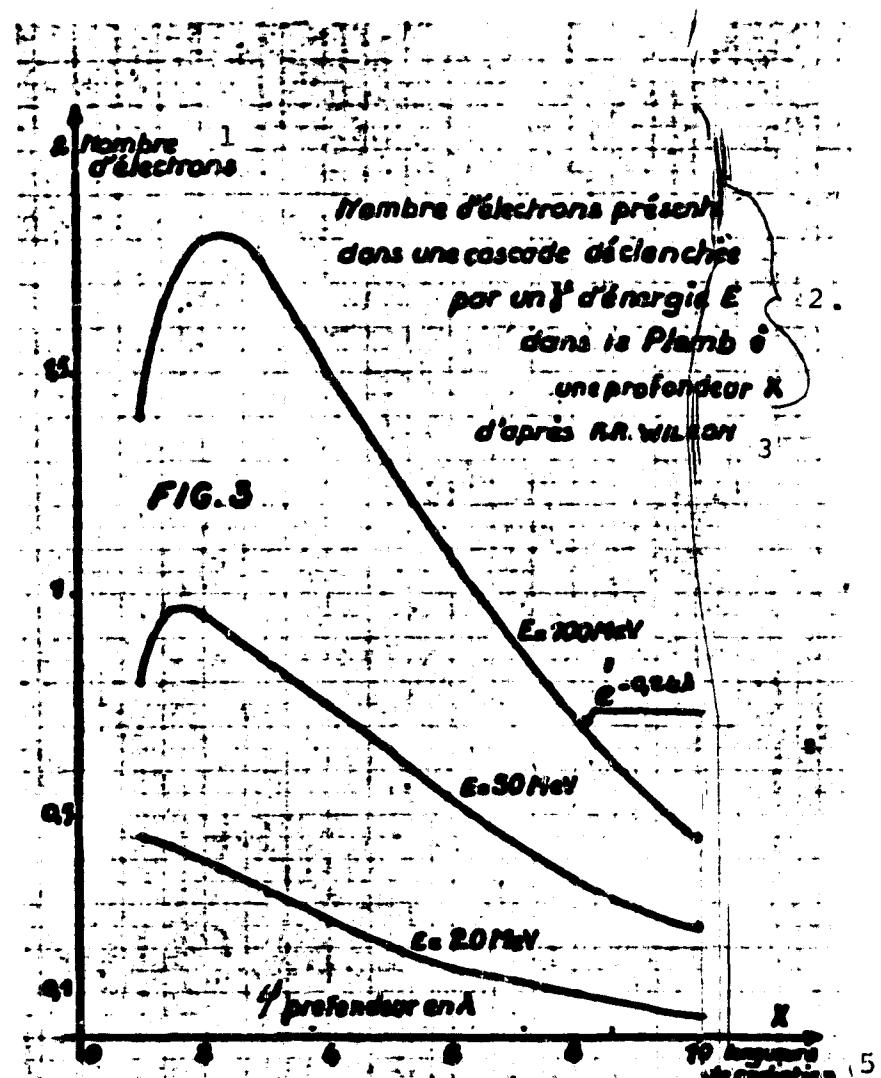
Figure 3

Key to Figure 3

1: Number of electrons 2: Number of electrons present in an avalanche
triggered by a γ of energy E in lead at a depth X 3: According to R.R.
Wilson 4: Depth in λ 5: Length of radiation

0.5 μs which did not allow us to concentrate the entire power of the /18
beam on the converter.

Remark: The current was measured in a 2% energy band as a function of
the energy of created particles.

CONCLUSION:

Even though the first experiments with the Faraday cup were promising ,
one should realize that it is difficult to use for measuring small currents
because the degassing of the graphite is slow. Since several weeks of
pumping are required to get stable readings and the installation only
has to be touched to change or exchange an element, this is a very
cumbersome procedure . Th addition of a valve and ion pump is not a remedy
because the high voltage of the pump disturbs the operation of the
sensor electronics and the valve reduces the angular acceptance. Another
promising solution consists of enclosing the graphite block except for the
lower part in a material like aluminium which does not degass. The
front part of the graphite can be coated or covered with mylar and
the Faraday cup operates at a low power.
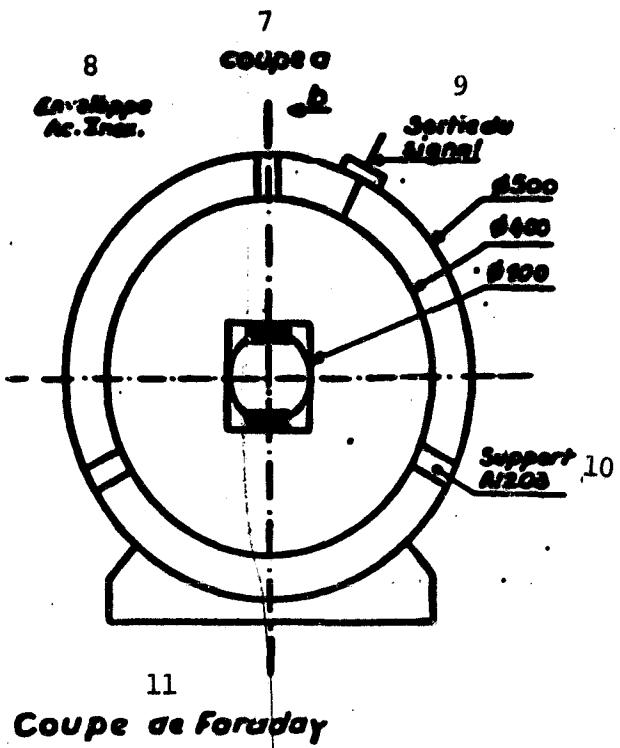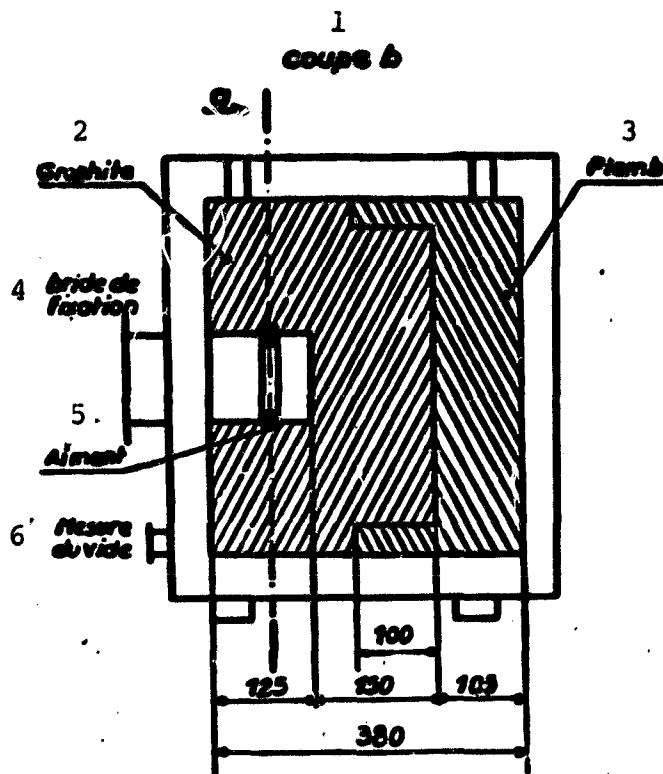
Figure 4

Figure 5

Key

1: Section b   2: Graphite   3: Lead   4: Attachment bracket   5: Magnet

6: Vacuum measurement   7: Section a   8: Stainless steel enclosure

9: Signal output   10: Support A1203   11: Faraday Cup
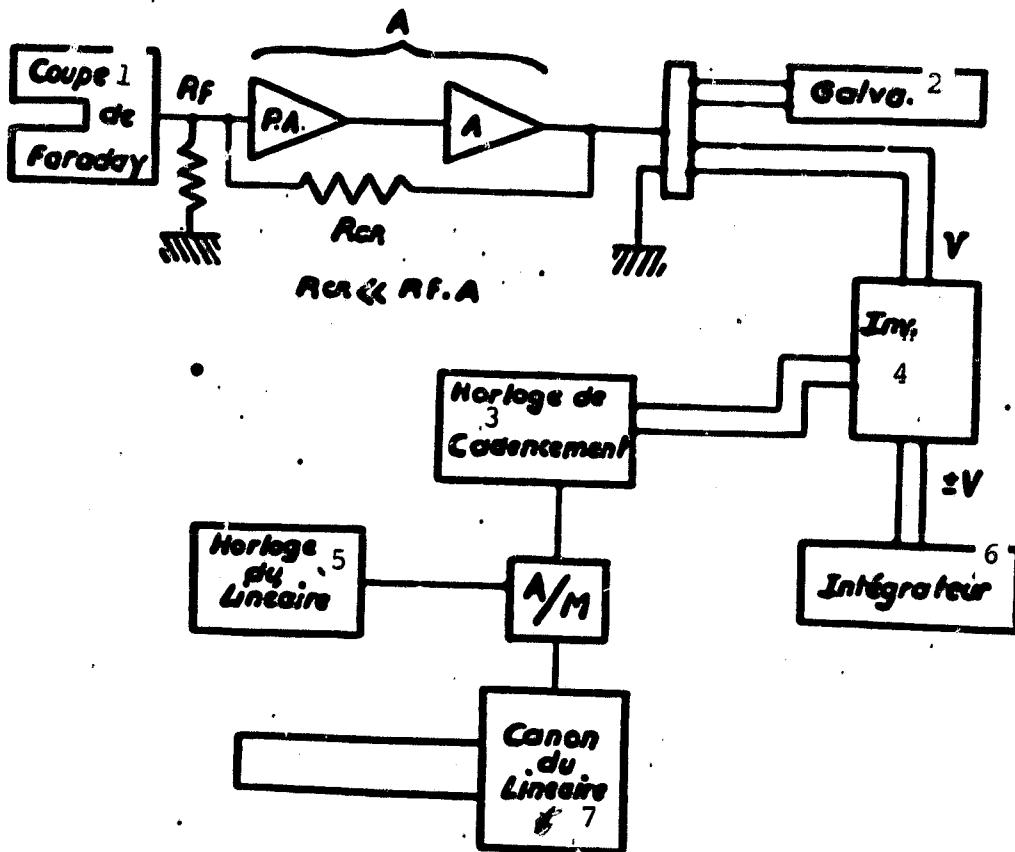
Figure 6

Key to Figure 6

1: Faraday cup   2: Galvanometer   3: Synchronization clock   6: Integrator

7: Linear accelerator gun
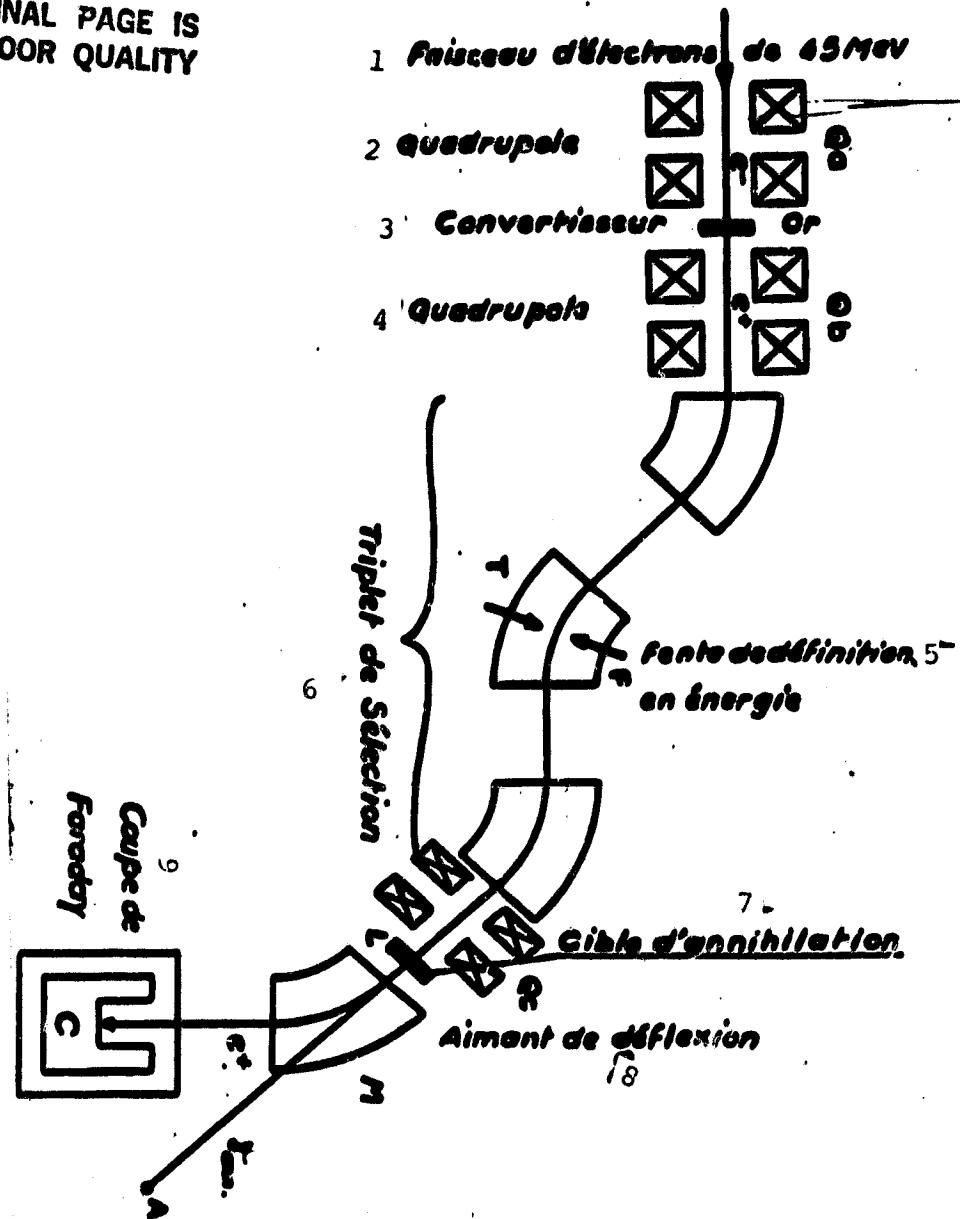
Figure 7

Key to Figure 7

1: Electron beam at 45 MeV   2: Quadrupole lens   3: Converter

4: Quadrupole lens   5: Energy determination slot   6: Triplet selection

lens   7: Annihilation target   8: Deflection magnet   9: Faraday Cup
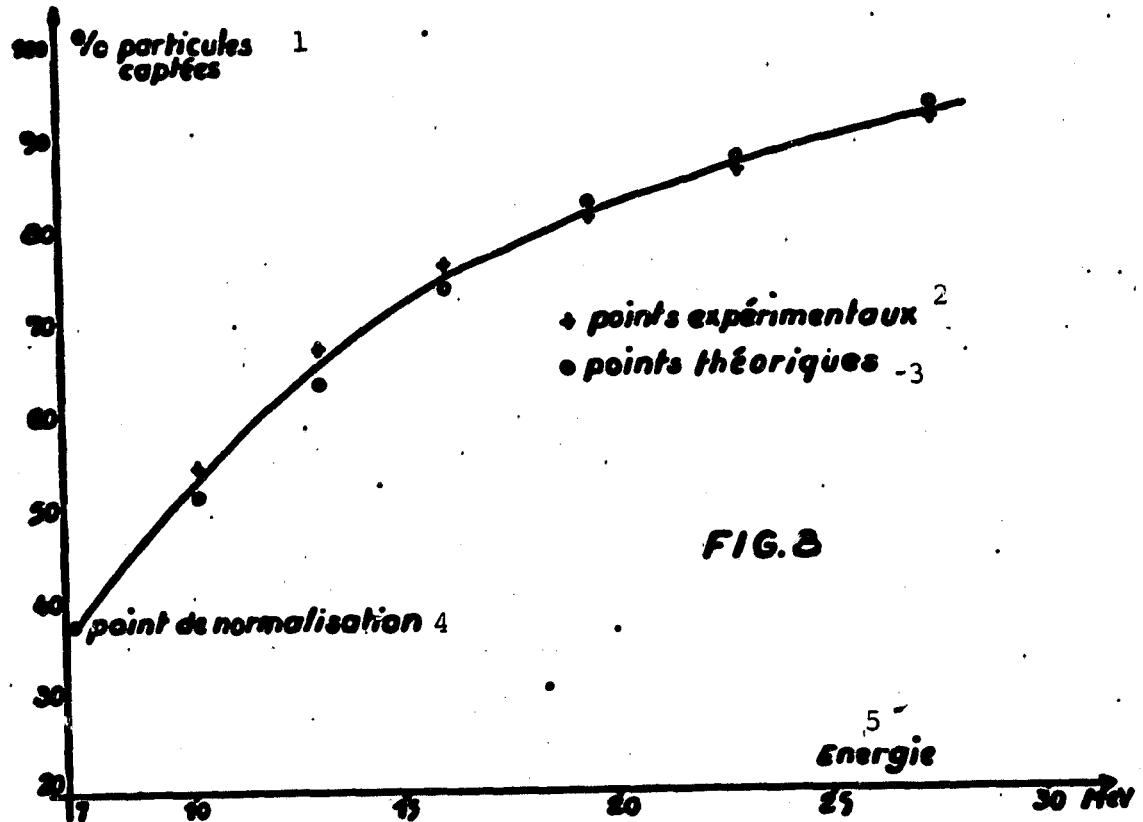
Figure 8

Key to Figure 8

1: Captured particles   2: Experimental points   3: Theoretical points

4: Standardization point   5: Energy
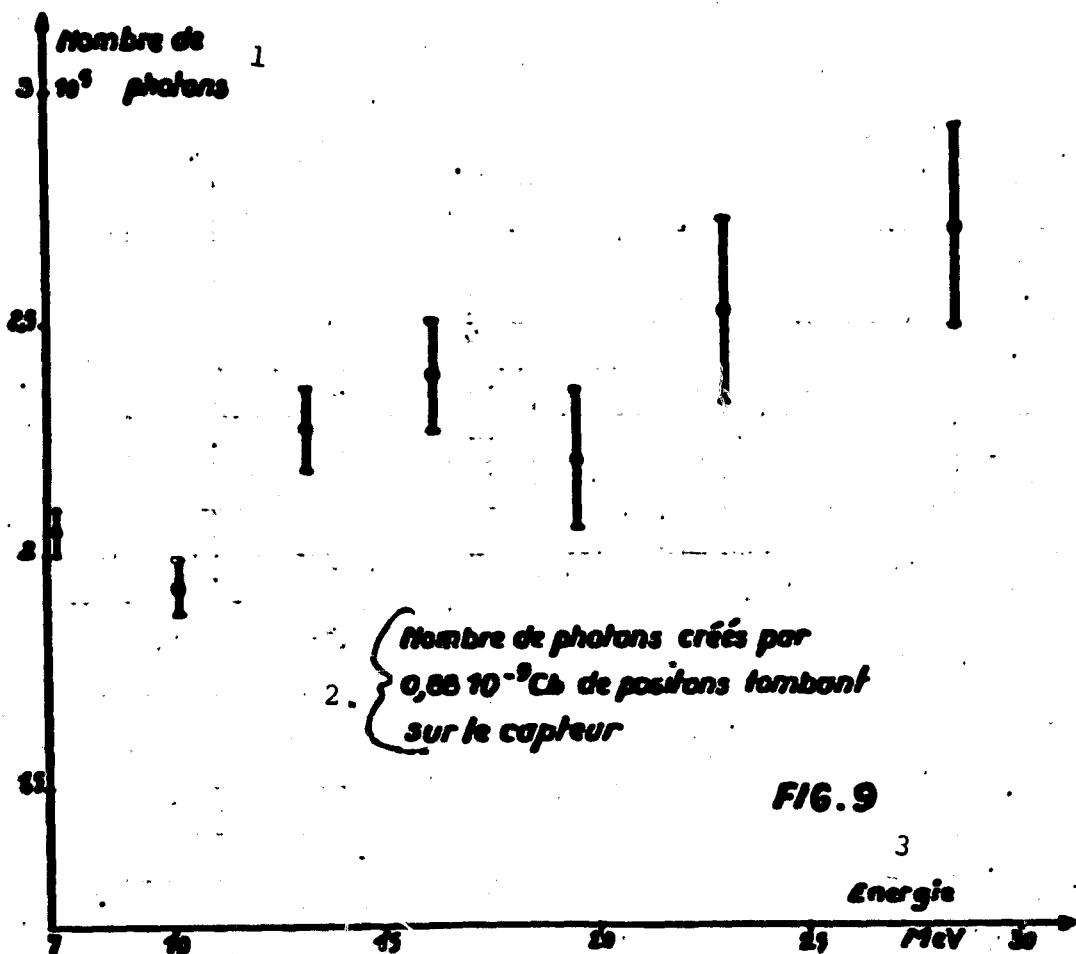
Figure 9

Key to Figure 9

1: Number of photons   2: Number of photons created by 0.88×10^{-19} Cb

positrons falling upon the detector   3: Energy
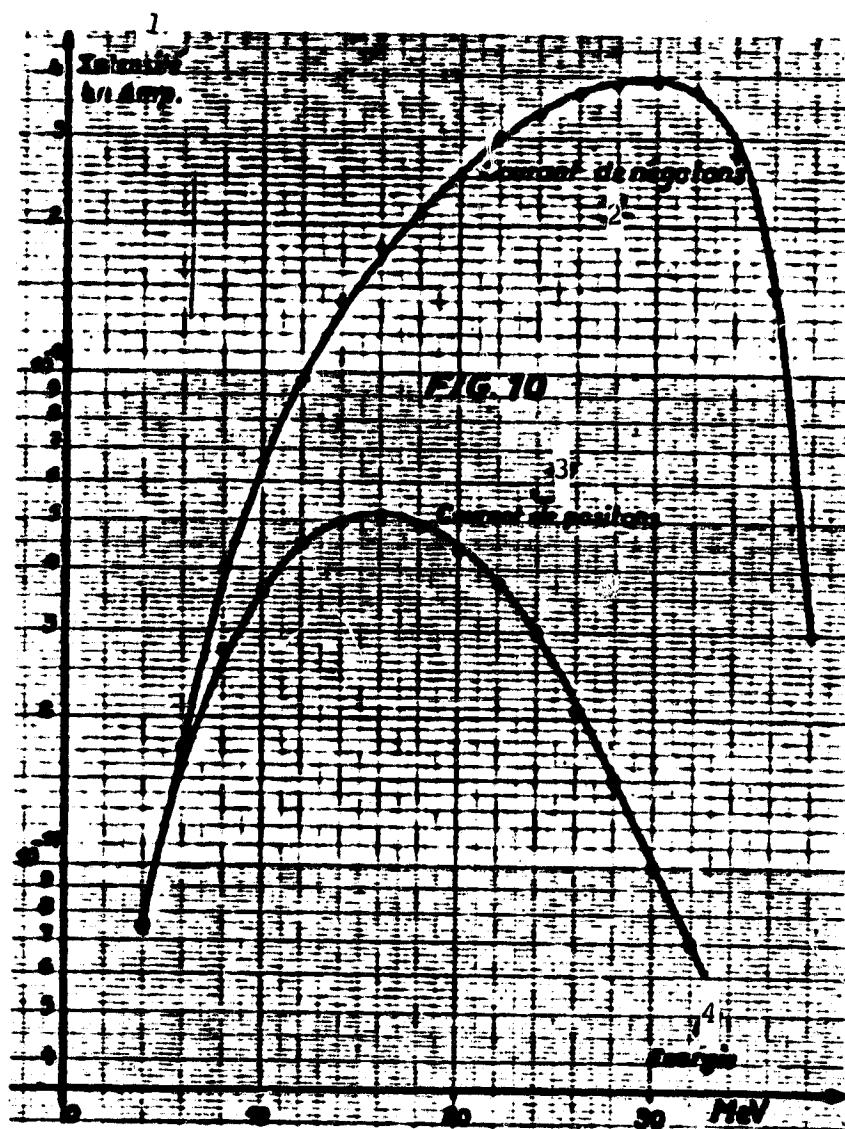
Figure 10

Key to Figure 10

1: Current in Amps   2: Negatron current   3: Positron current   4: Energy
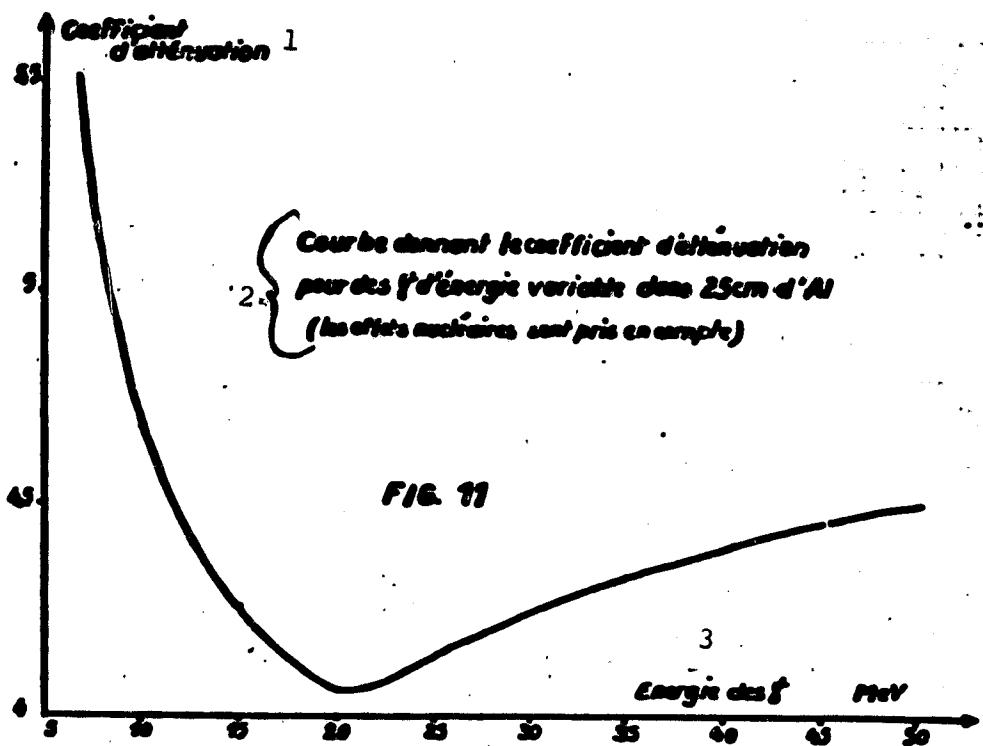
Figure 11

Key to Figure 11

1: Attenuation coefficient   2: Curve giving the attenuation coefficient
for γ of variable energy in 25 cm of Al (nuclear effects are taken into
account)   3: Energy of the γ
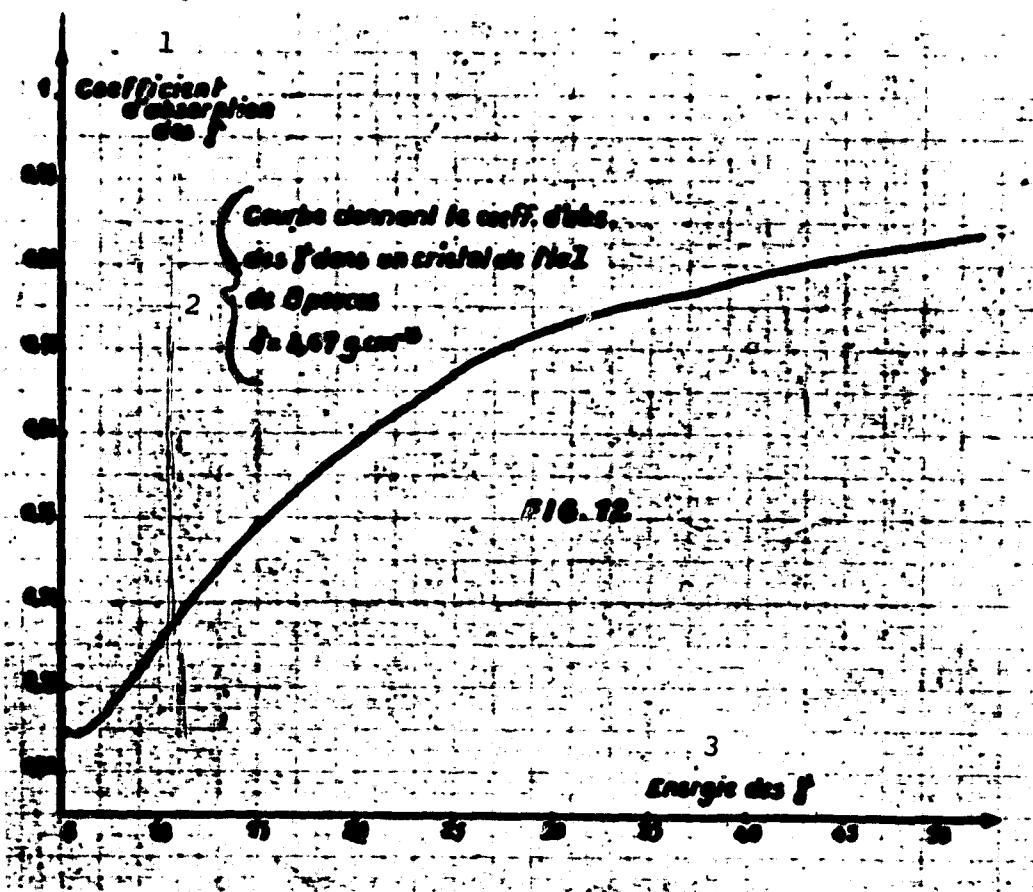
Figure 12

Key to Figure 12

1: Absorption coefficient of the γ 2: Curve giving the absorption
coefficient of the γ in an eight-inch NaI crystal, $d = 3.67$ g.cm^{-3}
3: Energy of the γ

REFERENCES

[1] C. Schuhl. Mesure de sections efficaces de photoproduction de neutrons en valeur absolue (Measurements of neutron photo-production cross-sections (absolute). Thesis Paris.

[2] J. Miller. La Resonance geante et les etats dipolaires des noyaux legers. (Disturbing resonance and dipolar states of light nucleii). Thesis Paris.

[3] G. Tamas, J. Miller, J. S. Schuhl, C. Tzara. Journal de Physique et le Radium 1960. 21. 532.

[4] E. Segre. Experimental Nuclear Physics. J. Wiley.

[5] M. J. Berger and S. M. Seltzer. Tables of energy losses and ranges of electrons and positrons. NASA, Washington, D. C.

[6] Production de photons de spectre etroit a partir d'electrons de grande energie. (Production of narrow spectrum photons from high energy electrons). Report C.E.A. No. 814, CEN Saclay.

[7] E. Fermi. Nuclear Physics--University of Chicago Press.

[8] R. R. Wilson. Monte Carlo study of shower production. The Physical Review vol. 86 no. 3, May 1, 1952.

[9] J. Kretschko, D. Harder and W.Pohlit. Absolutmessung der Teilchenflussdichte schneller elektronen mit einem Faraday-Kafig (Absolute particle flux measurements of fast electrons with a Faraday cup). N.I.M. 16 (1962) 29/36.

[10] K. L. Brown and G. W. Tautfest. Faraday Cup Monitors for high energy electron beams. The R.S.I. Vol. 27, No. 9, Sept. 1956.

[11] D. J. Gibbsons. Handbook of Vacuum Physics. Pergammon Press.

[12] H. Bruining. Physics and applications of secondary emission. Pergammon Press.

[13] R. O. Jenkins and W. G. Trodden. Electron and Ion Emission from solids. Routledge and Kegan Paul.

[14] A. J. Debber. Solid state physics Vol. VI--Academic Press.

[15] S. A. Blankenburg, J. K. Cobb, J. S. Moray. Efficiency of Secondary electron emission monitors for 70 MeV electrons. N.I.M. 39 (1966) 303-308.

[13] R. O. Jenkins and W. G. Trodden. Electron and ion emission from solids. Routledge and Kegan Paul.

[14] A. J. Debber. Solid state physics Vol. VI--Academic Press.

[15] S. A. Blankenburg, J. K. Cobb, J. S. Moruy. Efficiency of secondary electron emission monitors for 70 MeV electrons. N.I.M. 39 (1966) 303-308.

[16] V. J. VanHuise and R. E. Van de Vijver. N.I.M. 15 (1962 63-68.

[17] D. B. Isabelle and P. H. Roy. Factors influencing the stability of a secondary electron monitor. N.I.M. 20 (1963) 17-20.

[18] Shigeru Okabe, Tatsuo Tabata and Rinsuke Ito. Anomalous emission in secondary emission beam monitors. N.I.M. 26, (1964) (349-350).

[19] A. Ladage. Energy dependence of secondary emission monitors between 10 MeV and 5 GeV. Rapport DESY 65/16 Hamburg.

[20] T. L. Aggson. The Secondary emission monitor. Laboratoire de l'accelerateur lineaire. Orsay France. LAI 1028 (1962).

[21] H. Frank. Z. Naturforschung 14 a, 1959, 249.

[22] D. Harder and H. Ferbert. Physics Letters vol. 9, no. 3 15/4/1964.

[23] D. Turck. Diplom-Arbeit (Masters thesis). Technischen Hochschule Darmstadt 1966 (in press).

[24] J. S. Pruitt. Secondary electron trajectories in a Faraday Cup magnetic field. N.I.M. 39 (1966) 329-334.

[25] J. Goldenberg and R. H. Pratt. Magnetic electron scattering from nuclei. Review of Modern Physics, vol. 38, no. 2, April 1966.

[26] Notice technique CEA de l'amplificateur AC 4 K 2. Thomson Houston document no. 226/66 August 66.

[27] E. J. Williams. Multiple scattering of fast electrons and alpha-particles. Physical Review 1940, vol. 58, p 292.

[28] K. Siegbahn. Beta and gamma ray spectroscopy. North Holland 1955, p. 4.

[29] G. White Grodstein. X-ray attenuation coefficients from 10 KeV to 100 MeV. N.B.S. report no. 583.

[30] M. Bernardini, J. Miller, G. Tamas, C. Schuhl, C. Tzara.
Mesure du rendement de conversion negaton-positon (Measurement
of negaton-positon conversion yield) Rapport C.E.A. no. 2212
CEN Saclay.

[31] C. Schuhl. Rapport C.E.A. no. 1800 (1961) CEN Saclay.